INTERNATIONAL JOURNAL OF AUTOMOTIVE AND MECHANICAL ENGINEERING
ISSN: 2229-8649 e-ISSN: 2180-1606
VOLUME 23, ISSUE 1, 2026, 13216 - 13233
DOI: https://doi.org/10.15282/ijame.23.1.2026.5.1003

RESEARCH ARTICLE

Optimization of neem biodiesel blends and hydrogen addition to improve compression ignition engine performance

D. S. Doifode[1,2]*, A. J. Keche[1]

[1]Mechanical Engineering Department, Maharashtra Institute of Technology, Aurangabad, 431010 Maharashtra, India
[2]Mechanical Engineering Department, SVKM's Institute of Technology, Dhule, 424001, Maharashtra, India

Abstract – This research investigates the effects of Neem biodiesel and hydrogen-enriched air on the emissions and performance of a common-rail direct-injection diesel engine operating under variable load conditions of 25%, 50%, 75%, and 100%. The aim is to improve engine efficiency and promote sustainable energy solutions. Several Neem biodiesel blends (B10-B30) were initially evaluated, and B15 was selected for comprehensive analysis due to its optimal performance. Hydrogen as a gaseous fuel was subsequently inducted into the inlet air at rates of 3.34 to 9.27 liters per minute to assess its influence on engine behavior. Key parameters, including Brake Thermal Efficiency (BTE), Brake Specific Fuel Consumption (BSFC), and emissions of carbon monoxide (CO), hydrocarbons (HC), and oxides of nitrogen (NOx), were analyzed. The B15 blend exhibited a BSFC of 0.27 kg/kWh and a BTE of 31.38% at full load. With hydrogen supplementation at 5.19 liters per minute, BTE increased to 33.31%, and BSFC decreased to 0.25 kg/kWh. NOx and CO emissions were reduced to 488 ppm and 0.04%, respectively, while HC emissions remained unchanged. Hydrogen's high flame speed and broad flammability range contributed to emission reductions; however, higher hydrogen levels led to higher NOx emissions, necessitating ongoing monitoring to comply with regulations. The artificial neural network model, trained on experimental data, was very good at predicting performance and emissions, suggesting it could be used for real-time combustion diagnostics and fuel optimization. In summary, adopting dual-fuel systems utilizing hydrogen and Neem biodiesel offers significant potential to reduce the environmental impact of diesel engines.

Article History
Received : 01 July 2025
Revised : 08 December 2025
Accepted : 08 January 2026
Published : 02 March 2026

Keywords
Neem seed oil
Biodiesel
Hydrogen energy
CI engine
ANN

1. Introduction

Increased energy use and greater reliance on conventional fuels are significant contributors to environmental degradation. The transportation industry plays a vital role in the country's economic development [1]. However, it produces greenhouse gas emissions and affects air quality. Therefore, there is a need to find cleaner and more sustainable energy sources. Biodiesel is a viable option because it is renewable, non-toxic, and biodegradable. In addition, it supports rural agriculture and can be used in an existing compression-ignition (CI) engine with minimal modifications. Depending on regional resource availability, sustainability goals, and economic considerations, various raw materials are used to produce biodiesel for a CI engine. Plant-derived oils, including soybean, canola, sunflower, and others, are often the main feedstocks. In addition, non-edible sources like neem, mahua, jatropha, Karanja, and castor are used to produce biodiesel [2]. Biodiesel can also be produced from animal fats such as fish oil, tallow, lard, and poultry fat. Recently, waste cooking oil has also been used for biodiesel production [3]. Microalgae systems are also used to produce sustainable fuels, including biodiesel, ethanol, methane, and hydrogen [4].

Neem oil is obtained from the seeds of the Neem tree. It is a reliable feedstock for biodiesel production. It would help the diesel engines to consume less fossil fuel, which is good for the environment and energy sustainability. Transesterification can convert neem oil into biodiesel, with an oil content of 30-40% [5]. Many investigations have shown that neem biodiesel meets important fuel quality standards [5, 6, 7]. Several studies have shown that blending neem biodiesel, especially at B10 and B20 levels, can improve engine performance. Also, these kinds of blends reduce hazardous emissions, such as hydrocarbons (HC), Carbon monoxide (CO), and oxides of nitrogen (NOx) [8, 9]. Neem biodiesel is a sustainable substitute for diesel fuel. However, it has higher viscosity and lower volatility, which adversely affect combustion performance, leading to decreased engine performance and increased fuel consumption. So, it necessitates more effective combustion strategies [10, 11]. The combination of Neem biodiesel with hydrogen induction represents an effective strategy to enhance combustion characteristics and improve the performance of CI engines [12]. It is because hydrogen is considered a vital next-generation fuel due to its high heating value, rapid combustion rate, and environmentally friendly combustion characteristics [13]. As global research and investment in hydrogen production and CI engine adaptation increase, hydrogen is emerging as a sustainable alternative to fossil fuels. Research indicates that hydrogen enrichment improves engine performance and reduces hazardous emissions, making it a feasible solution for cleaner, more efficient combustion systems. Researchers have typically viewed neem biodiesel and hydrogen as separate alternative fuels. However, there are few extensive studies on their combined use in the CI engine. Table 1 gives the advantages of biodiesel, hydrogen, and the combined biodiesel-hydrogen methods as alternative fuels for the CI engine.

Table 1. Basic advantages of biodiesel, hydrogen, and their synergistic use in CI engine

*CORRESPONDING AUTHOR | Dattatray S. Doifode | ✉ dattatraya.doifode@svkm.ac.in

Advantage	Advantages of using biodiesel	Advantages of using hydrogen	Advantages of biodiesel and hydrogen combination
Biodegradable	✓	–	Partially
Renewability	✓	✓	✓
More Energy Density	–	✓	✓
Lower Emissions	✓	✓	✓
Safe handling	✓	–	✓
Engine Compatibility	✓	✓	✓
Improved Combustion	–	✓	✓
Reduced Carbon Footprint	✓	✓	✓
Supports Green Technology Transition	✓	✓	✓
Enhanced Fuel Flexibility	✓	✓	✓

Artificial Neural Networks (ANNs) are now useful tools for measuring engine performance. It can capture complex relationships between engine variables and their resulting parameters. Because of this, they can reliably predict important parameters such as brake-specific fuel consumption (BSFC), brake thermal efficiency (BTE), and various emission parameters. Studies show that ANN models can closely match experimental data, with correlation coefficients as high as 0.9998 and mean absolute percentage errors below 5%. Their high accuracy makes them very useful for engine performance and emissions analysis, as they reduce the need for extensive experimental trials [14, 15, 16]. The novelty of the present work is in the combined experimental and ANN-based analysis of Neem biodiesel–hydrogen dual-fuel operation in a common rail direct injection (CRDI) diesel engine under variable loading. Unlike previous studies, this work systematically optimizes biodiesel blending, hydrogen flow rate, and injection parameters while employing ANN modeling to predict performance and emissions, thereby addressing a critical gap in dual-fuel CI engine research. Improving these parameters can significantly increase combustion efficiency while reducing emissions.

This study aims to address several important objectives to fill a common gap in current research. Initially, to optimize fuel injection pressure and timing, various neem biodiesel blends (B10-B30) are systematically evaluated through thorough testing in an advanced diesel engine system. Subsequently, we analyze the effect of hydrogen induction at different combinations on the most promising blend to enhance the engine efficiency and reduce harmful exhaust emissions. Lastly, we develop and refine an ANN model to accurately predict the behavior of biodiesel-hydrogen combinations, with particular attention to engine efficiency and emissions. The overarching aim is to contribute toward a sustainable energy future by integrating environmentally friendly neem biodiesel with hydrogen, promoting more efficient diesel engine operation, and supporting the worldwide transformation to sustainable energy sources. Table 2 provides an extensive overview of significant research efforts investigating the performance of neem biodiesel in CI engines. The summary of Table 2 indicates that Neem biodiesel for diesel engines has yielded encouraging results. It enhances engine performance, as evidenced by improved BTE and decreased BSFC, and lowers environmentally undesirable emissions such as HC, CO, and smoke. The more favorable results are particularly notable when blended between B10 and B20. Neem biodiesel stands out as a more favorable and sustainable alternative to traditional fossil fuels for diesel engines, paving the way for a sustainable energy future. Additionally, Table 3 provides an extensive overview of the use of hydrogen-enriched biodiesel as a substitute energy source in CI engines.

The summary of Table 3 indicates that when hydrogen is injected in a limited and controlled manner with biodiesel, performance improves and CO and HC emissions are reduced, but to control NOx, other strategies are required. Based on the above literature, it is expected to optimize the performance of the CI engine in terms of BTE and BSFC, and to reduce CO and HC emissions when Neem biodiesel is used in combination with hydrogen gas in a dual-fuel mode. The inherently high diffusivity and fast flame propagation of hydrogen can mitigate the higher viscosity of Neem biodiesel fuel and promote complete combustion, thereby improving BTE and reducing BSFC. It is also hypothesized to reduce HC and CO emissions and maintain NOx levels by controlling hydrogen flow rates and various engine parameters, such as load, injection pressure, and injection timing.

2. Materials and Methods

2.1 Fuel Characteristics of Neem Biodiesel–Diesel Blends

Neem oil was selected as the basic base material for biodiesel generation. It is a non-edible resource and readily available in nature. The transesterification process was used to produce biodiesel using methanol and sodium hydroxide as catalysts. Main parameters, such as the temperature maintained between 55 and 60°C, the 3:1 molar ratio of methanol to neem oil, and the reaction duration, were carefully selected [3, 25, 26]. The biodiesel was filtered and thoroughly washed after the reaction to remove residual glycerol and other impurities. Each of the fuel blends of B10, B15, B20, B25, and B30 was carefully prepared and allowed to age at room temperature, as illustrated in Figure 1.

Table 2. Literature regarding the use of Neem biodiesel fuel in CI engine

CI engine with its Operational Parameters	Fuel Type and blend	Performance Result in (%)	Emission Result in (%)	Ref.
5.2, 1500 rpm, 17.5:1 compression ratio	Diesel, B25 (Neem), B25+MnO (100 ppm), B25+$FeCl_3$ (100 ppm)	BTE ↑ (up to 4%), BSFC ↓	CO ↓, NOx ↓, HC ↓, and smoke ↓ with nano-enhanced fuels	[10]
1500 rpm, 5.2 kW, 17:1 compression ratio	Diesel, B10, B15, B20 (Neem)	For B15, BTE ↑ (up to 27.73%), BSFC ↓	For B10, B15, and B20: CO ↓ (2.58%, 24.71%, and 18.66%), HC ↓ (26.77%, 8.63%, and 5.75%), NOx ↑ (24.56%, 34.68%, and 41.16%), Smoke ↓ (19.11%, 27.94%, and 38.23%)	[8]
5.2 KW, 1500 rpm, water-cooled, eddy current dynamometer, load variation: 20%, 40%, 60%, 80%, 100%; fuel flow and emission monitored using AVL instruments.	D80B20, D60B20E20, B80E20, B100, D100	D80B20: BTE ↑ 8.49% D60B20E20: BTE ↑4.25% B80E20: BTE↑ 3.02%, BSFC ↓	Smoke: ↓ D100 > B80E20, CO: ↓ D100 > B80E20, HC: ↓ D100 > B100, NOx: ↑ D100 < B100	[17]
Power = 4.4 kW at 1500 rpm Load range: 0% to 100% I.P.: 205 bars	Diesel of 40% + Neem biodiesel 40% + Ethanol 20% + 25 ppm Al_2O_3	BTE ↑ up to 7.2 % and BSFC ↓ 6.7 % with 25 ppm of alumina	CO ↓, HC ↓, NOx ↓ 17.49%	[18]
Kirloskar TV1, compression ratio of 17.5, 1500 rpm, Load = 0 to 100% at 25% steps	D90+JB5+NB5 (Diesel 90%, Jatropha 5%, Neem 5%)	Avg. BTE ↓ by 5.2%, Mechanical Efficiency: ↓ 9.79%, Volumetric Efficiency: ↓ 2.59% Avg. increase in: BSEC: 3.93%, EGT: 9.94%	For (D90 + NB5) CO_2 ↑ by avg. 8.75%, CO up to 46.91%, HC ↑ by avg. 0.34%, NO_x ↑ by avg. 16.56% compared to neat diesel	[2]
Vertical Engine, CR: 16.5–18.5:1, 3.5 kW at Speed: 1500 RPM, I.P.: 200 bars, Load: 25%–100%	Diesel + Neem-Castor oil (50:50) at B10, B20, B30	B30 showed the highest BTE, the lowest BSFC, and the highest Efficiency ↑ with blend %	Emission values not quantified	[19]
1.9 Multijet, CR: 18.3, 136 H.P., Max. Speed: 4200 RPM, Load: full load	B0 (Pure Diesel) NB5 (5% Neem ME + 95% Diesel) NB10 (10% Neem ME + 90% Diesel) CB5 (5% Camelina ME + 95% Diesel) CB10 (10% Camelina ME + 90% Diesel)	BSFC Increase: NB5: 0.95% CB5: 2.00% NB10: 1.67% CB10: 3.83%	CO ↓ by 4.4% to 12.09% HC↓ by 6.48% to 20.37% NOx ↑ 3.14% to 19.78%	[7]
Kirloskar Engine, 3.5 kW @ 1500 RPM, CR: 18:1, variable load.	Neem biodiesel blends (B10, B20, B30)	BTE ↑ by 34% (B10 over diesel) BSFC ↑ with higher blends	CO ↓ by 26%, HC ↓ by 17%, NOx ↓ by 21.875%, Smoke ↑ by 12% (For B10)	[20]

Meanings of Symbols Used in Table 2
"↓": Decrease / Lower value
"↑": Increase / Higher value

Table 3. Literature on the use of hydrogen-added biodiesel fuels in CI engines

4-Stroke C.I. Engine and Its Operational Parameters	Fuel Type and blend	Performance Result in (%)	Emission Result in (%)	Ref.
3.7 1500 RPM, 16.5:1 compression ratio, varying brake loads, I.P. 200-225 bar	WSLO20 + 25% H_2, WSLO40	For WSLO20 BTE ↑ 17.7% vs baseline For WSLO40, BTE ↓13.28%	NOx ↑22%, CO↓, HC ↓25%	[21]
1500 rpm, 550 cc, 3.7 kW, 17.5:1 compression ratio, different loads	B20 CNSL + H_2 (4, 8, 12 lpm) + Ethanol (5%, 10%, 15%)	Max BTE: 37.9% (↑ 6.5% vs diesel at 33.6%)	CO: ↓ 54.5%, HC: ↓ 7.4%, NOx: ↑ 34% (all vs diesel at full load)	[22]
(YANMAR L100V), 16.5:1 CR, 1500 rpm, full load	Juli flora biodiesel (B20) + H_2 (16 LPM) + 1000 ppm MA additive	BTE ↑ 28.81% (base), 2.17% with additive	NOx ↓ 21.9% (vs. B20+H_2), CO ↑ 9%, HC ↑ 2.4%	[23]
Engine speed: 18–30 rps; pilot fuel injection timing: 20–45° BTDC; (CR): up to 22; hydrogen flow rate: 0–18.04 LPM.	Waste Cooking Oil Biodiesel + Hydrogen (0–18.4LPM)	BTE ↑ 4.15%	CO ↓ 64.7%, NOx ↑ 76.61%, Opacity ↓ 57%	[3]
4.4 kW of power at 1500 rpm, CR = 18.5, FIP 220 bar	Diesel, JME20 + HHO gas	BTE ↑ 5.8%	HC ↓ 33.4%, CO ↓ 29.4%, NO ↑ 19.6%, Smoke ↓ 18.7%	[24]
CRDI, 1500 rpm, 80% load, Injection timing: 10° aTDC, Duration: 60° CA, Compression Ratio: 17.5	Diesel/Neem OME + Producer Gas + Hydrogen (6–12 lpm)	BTE improved to 28% (Diesel) and 23% (Neem OME)	CO ↓ 25.4%, HC ↓ 14.6%, Smoke ↓ 54.6%, NOx ↓ 26.8% (at optimal condition)	[12]
1500 rpm, variable load	CNSL B20 + H_2 (6 lpm) + DEE (2%, 4%, 6%)	BTE ↑ up to 37%; BSFC ↓ up to 45%	HC ↓ 43%, CO ↓ 50%, NOx ↑ 31%	[25]
3.5 kW at 1500 rpm, CR 17.5:1, IOP: 200, 220, 240 bars	B20 (Cottonseed biodiesel) + 15 lpm H_2	Max BTE: 33.60% at 220 bar (↑16% over diesel), BSFC ↓37%	HC ↓ 39% (from 123 ppm to 75 ppm), CO ↓ 33% (to 0.022% vol), NOx ↑ 18% (to 1254 ppm)	[13]
Kirloskar, 5.7 kW of power at 1500 rpm.	Full load, Hydrogen: 4 LPM via intake, Main fuel: TME + Ethanol (10%, 20%, 30%)	BTE ↑ 11.65%, 11.65%, 11.65%, 11.65%,10.87% and 7.58%	Major changes in CO ↓ 21%, CO_2 ↑ 14%, HC ↓ 19%, Smoke ↓ 22.45%, NOx ↓ 17.03%	[26]

Meanings of Symbols Used in Table 3
"↓": Decrease / Lower value
"↑": Increase / Higher value

The properties of these mixed fuels, including density, heating value, flash point, fire point, and viscosity, were analyzed using standard methods outlined by ASTM D287, ASTM D4809, ASTM D93-58T, ASTM D93-58T, and ASTM D444, respectively. Table 4 provides details of the fuel properties of various Neem biodiesel blends and diesel fuel, evaluated at Apex Innovations Pvt. Ltd., Sangli, India, in accordance with the American Society for Testing and Materials (ASTM) standard.

Figure 1. Pure diesel and Neem biodiesel blend samples were used in experimental testing

Table 4. Fuel properties of pure diesel and Neem biodiesel blends were determined as per the ASTM standard

Sample/Properties	Density at 25°C	Calorific Value of Blend	Flash Point	Fire Point	Kinematic Viscosity at 40°C	Dynamic Viscosity at 40°C
Unit	Kg/m³	KJ/Kg	O_c	O_c	cSt	cP
Standard of ASTM	D287	D 4809	D 93-58T	D 93-58T	D445	D445
Std. Diesel	816	45448	53	56	2.09	1.73
B10	824	45184	62	66	2.35	1.93
B15	829	44810	65	69	2.43	2.01
B20	833	44516	69	74	2.66	2.21
B25	834	44230	73	79	2.74	2.28
B30	839	43739	76	82	2.86	2.39
B100	851	39709	125	141	4.20	3.57

2.2 Experimental Arrangement

Figure 2 shows a single-cylinder, four-stroke, water-cooled CRDI diesel engine used in the experimentation. It features an innovative, common-rail, high-pressure fuel-injection system and an electromagnetic eddy-current dynamometer. The measurement setup comprises instruments for measuring load, temperature, air intake, fuel use, crank angle, combustion chamber pressure, etc. It is equipped with a data-acquisition system interfaced directly to a computer. There is a special panel on the setup that holds an air box, two fuel tanks, a fuel measurement device, a manometer, flow transmitters for fuel and air, a process indicator, and a piezoelectric power unit. Using rotameters, water flow rates can be measured precisely for the calorimeter and the engine. This engine has an open, programmable Electronic Control Unit (ECU) designed for precise diesel fuel injection. It also includes a fuel injector, a standard rail system, a rail pressure sensor, a crank position sensor, a pressure-regulating valve, and a complete electrical wiring system. Table 5 lists the technical specifications of the test setup. An AVL five-gas analyzer is used to measure exhaust emissions like HC, CO, CO_2, O_2, and NOx, as shown in Figure 3. Their resolution and measurement range are shown in Table 6.

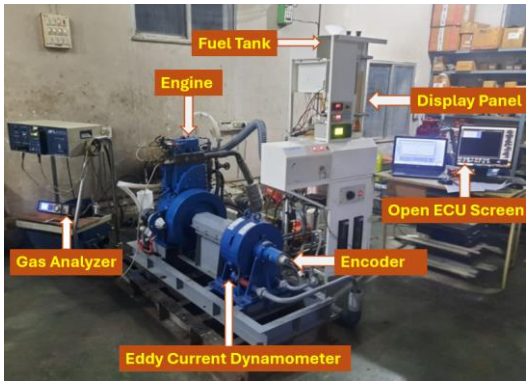

Figure 2. Experimental engine setup with all the accessories

Table 5. Technical specifications of the test setup

Parameters	Description
Type of Engine	Kirloskar, 1 cylinder, 4-stroke, water-cooled
Power and speed	3.5 kW at 1500 rpm
Cylinder Bore and Stroke	87.5 mm and 110 mm
Dynamometer	Eddy current Type
Compression ratio	17.5:1
Fuel Tank Capacity	15 Liters with dual compartments
Piezo powering unit	Cuadra Make and Model AX-409
Injector Type	Solenoid driven
Common rail	Modified common rail, with pressure sensor
Piezo sensor	Combustion: Range 350 bar with low-noise cable
Angle of Crank Sensor	Resolution is 1 degree with the TDC pulse.
Fuel injection pressure	800 Bar
Fuel Injection timing	210 (Before top dead center) BTDC

Figure 3. AVL DIGAS 444 Exhaust Gas Analyzer and 437 Smoke Meter used for emissions measurement

Table 6. Specification of AVL DIGAS 444 exhaust gas analyzer

Item	Technical specifications
Name of Device	Automotive Exhaust Gas Analyzer
Resolution	HC and NOx of 1 ppm, CO_2 of 0.1% Vol., O_2 of 0.01% Vol., and CO of 0.001% Vol.
Measurement Range	HC from 0 to 20,000 ppm of Vol., CO_2 (0 to 20% Vol.), CO from 0 to 15% of Vol., and NOx from 0 to 5,000 ppm Vol.

2.3 Important Devices Used in The Hydrogen Fuel Supply System

The intake manifold was supplied with hydrogen gas to inject hydrogen-rich air into the combustion chamber. Figure 4 shows that this system includes a hydrogen tank, a pressure gas regulator, a flow gas meter, a flame-trapping device, and an electronic control unit. A flame trap is a safety device that prevents the propagation of flames. A pressure-reducing device delivered hydrogen at about 2 bars. To ensure optimal performance, the flow meter carefully controlled the hydrogen flow rate.

2.4 Experimental Procedure Followed

Initially, pure diesel was tested in a CI engine at loads of 25%, 50%, 75%, and 100% at a compression ratio of 17.5. For different loads, the engine's brake power is obtained. Its performance and emission results were used as a base for comparison with further testing of various blends of Neem biodiesel, like B10, B15, B20, B25, and B30, and different flow rates of hydrogen gas, like 3.34, 5.19, 6.12, 7.42, and 9.27 liters per minute (L/min). Similarly, each biodiesel blend, ranging from B10 to B30, was independently tested under increasing engine load. A comparison with pure diesel was conducted to determine the optimal biodiesel blend. The blends that demonstrated the highest BTE efficiency and the lowest emissions were selected as the optimum blend. Subsequently, hydrogen gas was supplied to the engine at various flow rates while the engine operated on a previously determined optimum blend of Neem biodiesel and diesel fuel. The engine was re-evaluated under the same load conditions for each hydrogen flow rate to examine how hydrogen enrichment affected performance and emissions. Finally, the best hydrogen flow rate for an optimum blend of Neem biodiesel can be

obtained. To ensure reliability and consistency, all measurements were repeated four times, and the average values were used for data analysis.

(a) Hydrogen supply cylinder with dual-stage pressure regulators

(b) Flame trap

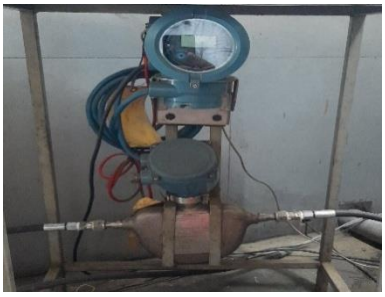

(c) Flow meter

(d) Electronic control unit

Figure 4. Photograph of the hydrogen fuel supply system components used for the experimental setup

2.5 Uncertainty Estimation

Quantifying uncertainty is an essential component of any scientific or engineering endeavor, as it directly influences the dependability and precision of the acquired results. These kinds of errors can come from several sources, such as the inherent limitations of measuring tools, environmental factors like vibrations, calibration issues, and problems with electrical or mechanical connections. So, an uncertainty analysis is necessary to check the data. The root-mean-square approach, as indicated in Eq. (1), is used to estimate uncertainty.

$$\Delta R = \sqrt{\left(\frac{\partial R}{\partial x_1}\Delta x_1\right)^2 + \left(\frac{\partial R}{\partial x_2}\Delta x_2\right)^2 + \cdots + \left(\frac{\partial R}{\partial x_n}\Delta x_n\right)^2} \quad (1)$$

Eq. (1) evaluates the uncertainty (ΔR) linked to a measurement that depends on 'n' independent variables (x_1, x_2, x_3, ..., x_n). Each of these variables introduces its own specific uncertainty (Δx_1, Δx_2, Δx_3, ..., Δx_n), corresponding to the different levels of variability inherent in each measurement. In our current investigation, the observed percentage uncertainties for main performance parameters and emission parameters, including BSFC, BTE, HC, CO, Carbon Dioxide (CO_2), and NO_x, were determined to be approximately 1.41%, 1.42%, 3.08%, 1%, 2%, and 1.93%, respectively. These figures support the robustness of our experimental results. Moreover, the overall uncertainty calculated for this research remains below ±5%, which aligns well with values reported in the existing literature, indicating the reliability of our findings [27, 28].

2.6 Artificial Neural Network Framework

The ANN framework was developed to accurately forecast performance parameters, such as BTE, BSFC, and emissions of NOx, CO, HC, CO_2, O_2, and smoke. The experimental data were obtained from a CI engine operated across a broad scope of loads, fuel blends, and hydrogen flow rates. An exploratory data analysis was performed before model development. It involved evaluating input and output variables, analyzing their distributions, assessing class imbalance, visualizing correlations, exploring skewness, creating histograms, and identifying outliers. Standard data cleansing procedures were implemented to ensure good data quality, addressing issues such as duplicate records, data conversion outliers, removals, and inconsistencies. The ANN model was developed using 100 experimental samples. A hold-out validation strategy was employed, where the data was split randomly into 70% for training, 20% for validation, and 10% for testing. The validation dataset was employed to tune parameters and to track model behavior during training to minimize overfitting, whereas a separate test dataset was reserved solely for assessing the final model's predictive performance. The validation framework ensures reliable generalization capability despite the limited dataset size. The

structured data division enables effective assessment of the model's learning ability and its predictive performance on previously unseen data, thereby enhancing model reliability.

Figure 5 illustrates the ANN model trained using the backpropagation algorithm to capture the nonlinear relationship between the input and the output parameters. It consists of an input layer with three neurons representing engine load, fuel blend ratio, and hydrogen flow rate. This is followed by two hidden layers, each with 25 neurons, the number determined empirically to achieve optimal predictive performance. The Adam optimizer with a learning rate of 0.0005 was selected for the training. The output layer has eight neurons aligned with the engine performance and emission parameters. The hidden layers use the Leaky ReLU activation function, which provides the nonlinear modeling capacity needed to analyze complex relationships in the data. Multiple network configurations were evaluated to achieve an optimal balance between predictive effectiveness and model complexity.

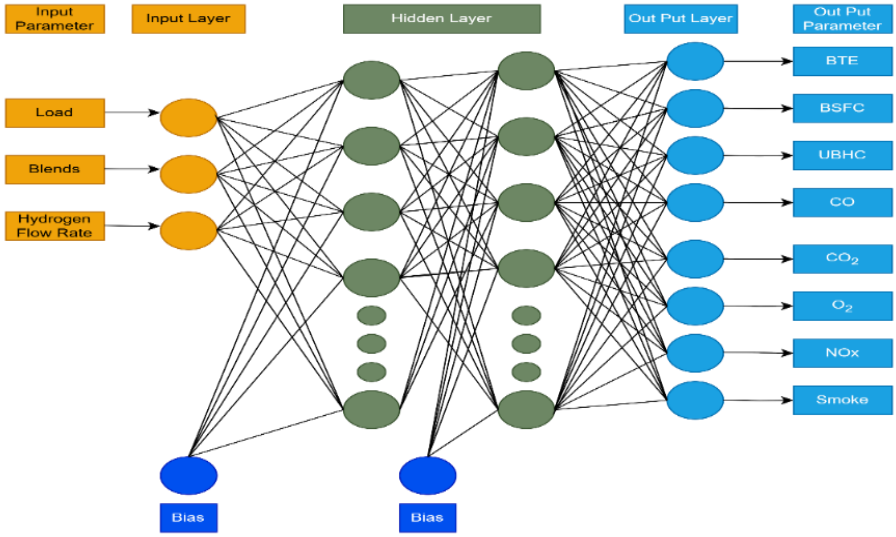

Figure 5. Architecture of the ANN model

2.7 Training of The Network

The ANN was trained, and backpropagation was performed in Python using algorithm optimization methods, such as the Adam optimizer. The mean squared error (MSE) was selected as the loss function. The average squared difference between predicted and actual values is quantified. The training lasts for several epochs until the model either converges or the validation loss improves. To make the model more stable and less prone to overfitting, approaches such as early stopping and learning rate scheduling were used. Model performance was evaluated using the correlation coefficient (R), mean squared error (MSE), and mean absolute percentage error (MAPE), as outlined in Eqs. (2-4) [29].

$$R = 1 - \frac{\sum_{i=1}^{N}(x_i - y_i)^2}{\sum_{i=1}^{N}(x_i - \bar{y}_i)^2} \tag{2}$$

$$MSE = \frac{1}{N}\sum_{i=1}^{N}(x_i - \bar{y}_i)^2 \tag{3}$$

$$MAPE = \frac{1}{N}\sum_{i=1}^{N}\left(\frac{x_i - y_i}{x_i}\right)X100 \tag{4}$$

where N = No. of samples tested, x_i = Measured (observed) values, y_i = Predicted value, and $\bar{y}_1$=Average of predicted values

3. Results and Discussion

An experimental analysis was conducted using five distinct Neem biodiesel-diesel blends, designated B10, B15, B20, B25, and B30. These tests were conducted with a consistent fuel injection timing set at 21° before top dead center and a fuel injection pressure of 800 bar, while increasing the engine load. Based on the loads, the respective brake powers are obtained. The data collected effectively illustrates the emerging trends in engine performance and emission characteristics across various fuel combinations.

3.1 Evaluation of Performance Metrics of The CI Engine for Neem Biodiesel–Diesel Fuel

Figure 6(a) shows a comparative evaluation of the BTE of biodiesel blends and diesel fuel. Among the blends evaluated, B15 achieves the highest BTE of 31.38%, which is lower than the 35.21% obtained for pure diesel. This marginal decrease

in efficiency for biodiesel blends is owing to their higher viscosity and lower calorific value, which affects combustion and overall energy conversion. In addition, it is observed that as brake power increases, BTE also increases. It means the engine shows better BTE at higher brake power. It is because of decreased relative heat losses, better combustion efficiency, and greater useful power output compared to frictional losses. Finally, it is concluded that B15 emerges as the most promising blend. It was also found that for the unmodified engine, higher blends are less suitable. The BSFC obtained after testing various Neem biodiesel-diesel fuels and pure diesel in a CI engine is shown in Figure 6(b). It shows that BSFC for all neem biodiesel blends decreases with increasing brake power. Among the tested blends, the lowest BSFC was obtained for B15. It is also stated that as the volume of neem biodiesel in the blend increases, the BSFC also increases. The observed trend is largely attributed to the lower calorific value and higher viscosity of neem biodiesel compared with pure diesel. It indicates that more fuel is required to produce the same amount of energy.

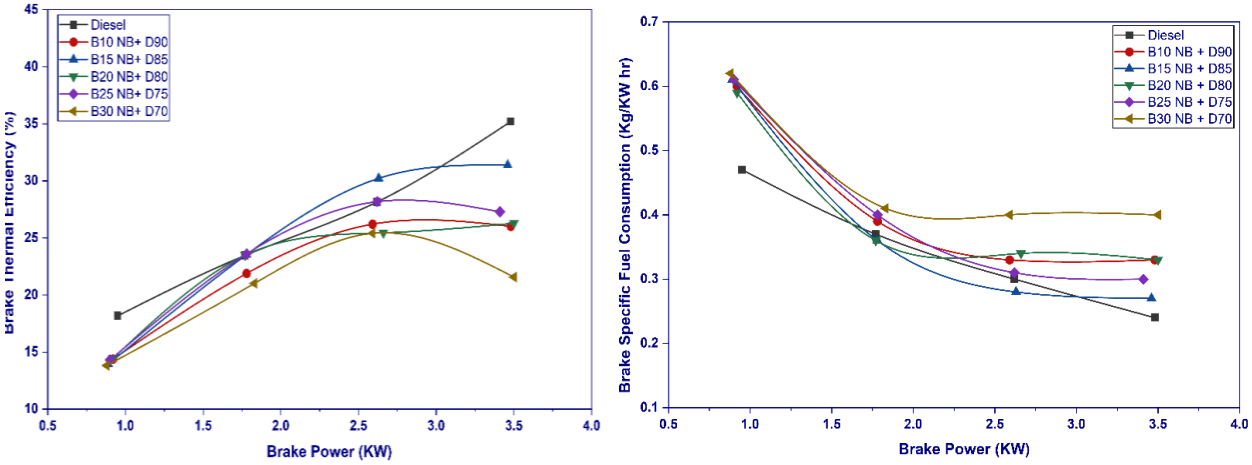

(a) Changes in BTE (b) Variation of BSFC

Figure 6. Engine performance characteristics for various Neem biodiesel and diesel fuel combinations

An increase in mechanical efficiency with brake power for various fuel combinations is shown in Figure 7(a). This is because output work increases relative to frictional losses at higher brake power. Diesel fuel shows the highest mechanical efficiency of 71.11%. Biodiesel blends also show a similar trend at higher brake power. Nevertheless, as the blend ratios increase further, mechanical efficiency decreases slightly. The observed effect is primarily due to higher viscosity and lower calorific value. Figure 7(b) shows that volumetric efficiency decreases to a smaller extent as brake power increases for different blends. This reduction is due to an increase in cylinder air temperature at higher engine load, which decreases the air density and the mass of air introduced into the engine cylinder. Compared with all the fuel blends, diesel fuel has the lowest volumetric efficiency due to its higher combustion temperature and lower density. On the other hand, all biodiesel blends exhibit better volumetric efficiency at lower loads due to their higher oxygen content and density, which enhance combustion and improve the utilization of introduced air.

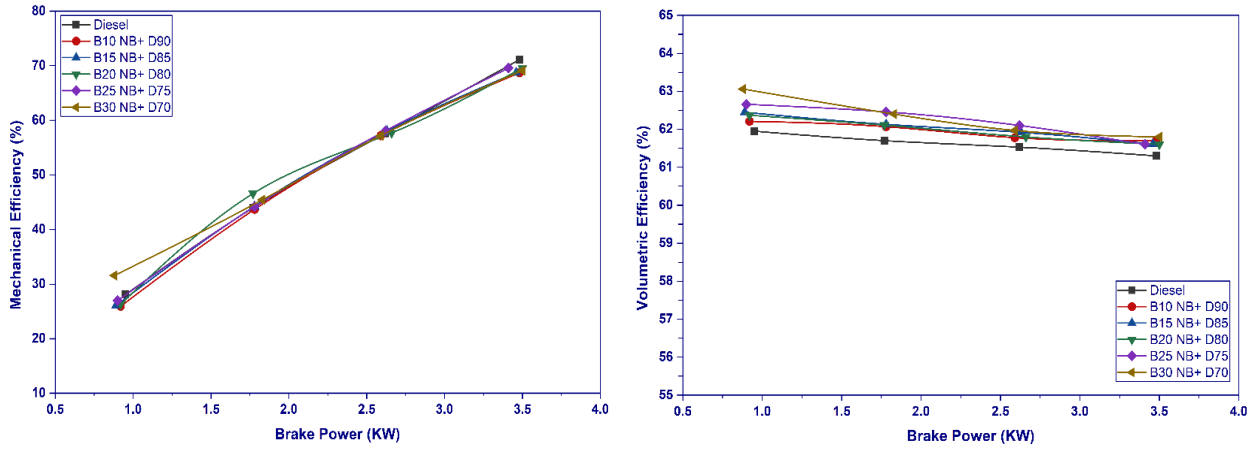

(a) Mechanical efficiency (b) Volumetric efficiency

Figure 7. Efficiency variations for various Neem biodiesel and diesel fuel combinations

Figure 8(a) shows the variation of cylinder pressure with crank angle for diesel and Neem biodiesel blends at full load. Neem biodiesel blends exhibit slightly earlier peak pressure than diesel due to a shorter ignition delay caused by their higher cetane number and oxygen content. Diesel recorded a maximum pressure of 66.05 bar at 371° ATDC, while

B10, B15, B20, B25, and B30 showed peak pressures of 64.72, 62.74, 60.76, 58.78, and 56.80 bar, respectively. The reduction in peak pressure with increasing biodiesel content is attributed to higher viscosity and poorer atomization. Peak pressure increases with engine load for all fuels. Figure 8(b) illustrates the variation of heat release rate with crank angle for diesel and Neem biodiesel blends. All blends exhibit combustion behavior like diesel, with diesel showing a peak heat release rate of 86.45 J/°CA, while B10 records 84.72 J/°CA. The peak heat release rate slightly decreases with increasing biodiesel content due to lower volatility, higher viscosity, reduced calorific value, and poorer atomization. The negative heat release region corresponds to the compression and pre-combustion phase caused by fuel vaporization and heat loss to the cylinder walls.

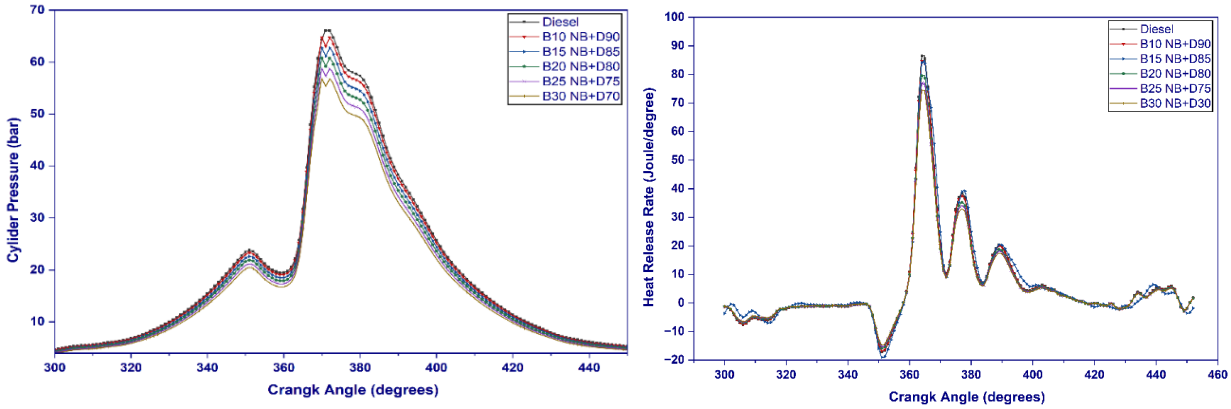

(a) Cylinder pressure (b) Heat release rate

Figure 8. Variation of cylinder pressure and heat release rate with crank angle for Neem biodiesel-diesel fuel blends.

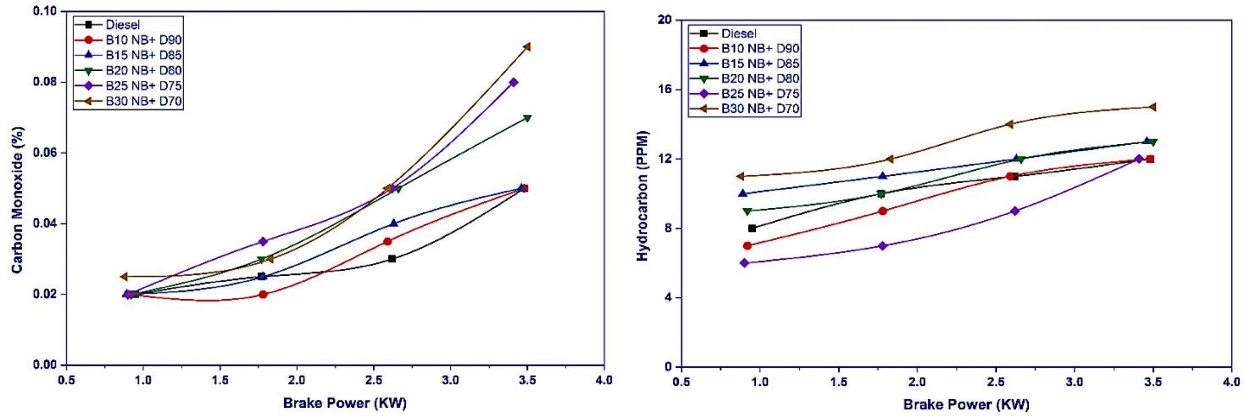

(a) Carbon monoxide (b) Hydrocarbons

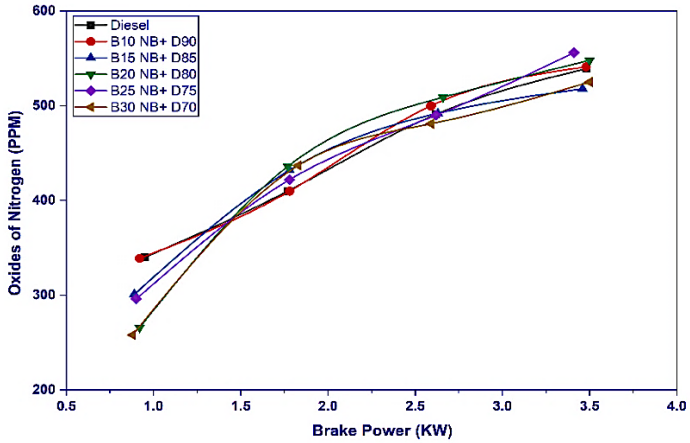

(c) Nitrogen oxides

Figure 9. Variation of exhaust emissions with brake power for Neem biodiesel blends and diesel fuel

3.2 Evaluation of Emission Parameters of CI Engine for Neem Biodiesel–Diesel Fuel

The increasing trend of CO emissions with brake power for various Neem biodiesel blends and diesel fuel is shown in Figure 9(a). Diesel produces the least CO emissions compared to biodiesel blends, especially at full load. The B10 and B15 blends produce about the same amount of CO as regular diesel. On the other hand, the B30 blend has the highest emissions of all the biodiesel blends. The main reason for this trend is that this blend is thick and less volatile, leading to less burning and less incomplete combustion of fuel. When the brake power is low, the changes in CO emissions are small. However, when the brake power is high, the fuel blend has a bigger effect on emissions. The data in Figure 9(b) show that HC emissions increase with brake power when various Neem biodiesel blends and diesel fuel are tested in a CI engine. This is because neem oil is thicker and less volatile, so it does not atomize well, and it leads to incomplete combustion. This leads to more unburned HC, especially at higher brake power. Also, greater volumes of fuel blends create richer mixture zones during combustion, which in turn produce more HC emissions. As shown in Figure 9(c), NO_x emissions rise with brake power across all fuel blends and pure diesel. This change occurred because of higher temperatures generated during combustion. The B15 biodiesel blend has the lowest NOx emissions (518 ppm), which is lower than diesel (539 ppm. It is due to the lower combustion temperature for the B15 blend compared to pure diesel. The other biodiesel blends also emit lower NOx compared to diesel. This is due to higher viscosity, poor atomization, and lower combustion temperatures observed with biodiesel blends. Overall, these results indicate that it is important to strike a balance between good combustion and minimizing NOx emissions, especially as more biodiesel is used.

3.3 Evaluation of Performance Parameters of CI Engine for Varying Hydrogen Flow Rate, Optimum Biodiesel Blend, and Diesel Fuel

When the engine was running on the B15 fuel at an optimal blend, hydrogen gas at standard temperature and pressure (STP) was inducted into the inlet manifold at the following flow rates: 3.34, 5.19, 6.12, 7.42, and 9.27 liters per minute (L/min). Its effect on engine performance was thoroughly examined across varying load scenarios. As shown in Figure 10(a), BTE increases with increasing brake power for all tested hydrogen flow rates and diesel fuel. This is because combustion is better at higher engine brake power. For B15 Neem biodiesel fuel without hydrogen, BTE was 31.38%. When B15 Neem biodiesel was combined with 5.19 L/min (liters per minute) of hydrogen and subjected to full load, its BTE reached its maximum value of 33.31%. The fundamental reason for this rise is that hydrogen burns more efficiently, with a higher flame speed and a broader flammability range. Hydrogen also has a higher calorific value. However, it was also found that the BTE decreased when the hydrogen flow rate was increased above 5.19 L/min. This was most likely caused by knocking and incomplete fuel combustion. During the testing, diesel consistently showed a slightly greater BTE than all other blends. These results indicate that optimizing hydrogen flow rates improves thermal efficiency while maintaining steady combustion conditions. A decreasing trend in BSFC with increasing brake power is observed for all hydrogen flow rates and diesel fuel. This pattern results from improved combustion efficiency and lower heat losses at higher brake power, as depicted in Figure 10(b). The B15 Neem biodiesel, with hydrogen flow rates between 5.19 and 9.27 L/min, had the lowest BSFC of all the fuel blends tested. It shows the most efficient fuel combinations because hydrogen combustion in the engine cylinder is more efficient. Whereas a lower hydrogen flow rate of 3.34 L/min significantly raises BSFC, because of improper combinations and mixing of fuel and air mixture. These results highlight the need to meticulously optimize hydrogen flow rates to improve fuel efficiency in dual-fuel engine systems.

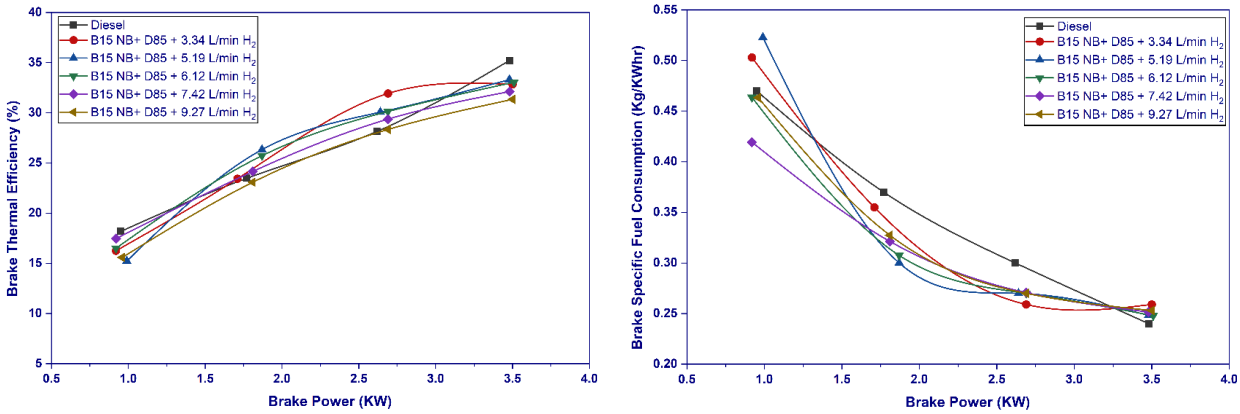

(a) Changes in BTE (b) Variation of BSFC

Figure 10. Engine performance characteristics for various hydrogen flow rates and Neem biodiesel-diesel fuel combinations

Mechanical efficiency increases with brake power across all tested hydrogen flow rates and diesel fuel, as depicted in Figure 11(a). This is mainly because of the reduction in relative frictional losses as the engine's brake power increases. The analysis also shows that biodiesel blends containing 15% Neem biodiesel work better than pure diesel when hydrogen is added. Improved combustion and smoother engine operation are achieved with hydrogen addition. Finally, it can be stated that adding the appropriate amount of hydrogen appears to slightly improve mechanical efficiency across a range

of loads from medium to high. Figure 11(b) shows a slight decrease in volumetric efficiency with increasing brake power due to reduced air density at higher cylinder temperatures. The B15 Neem biodiesel with a hydrogen gas flow rate of 5.19 L/min achieved the highest volumetric efficiency of 61.75% among all hydrogen flow rates. This is because it displaces less air and has lower hydrogen volume. On the other hand, higher hydrogen flow rates decrease the volumetric efficiency by pushing more oxygen-rich intake air due to excess hydrogen. Diesel fuel maintains constant efficiency, providing a reliable baseline. Overall, hydrogen enrichment slightly affects volumetric efficiency, but at higher hydrogen flow rates, optimization is required.

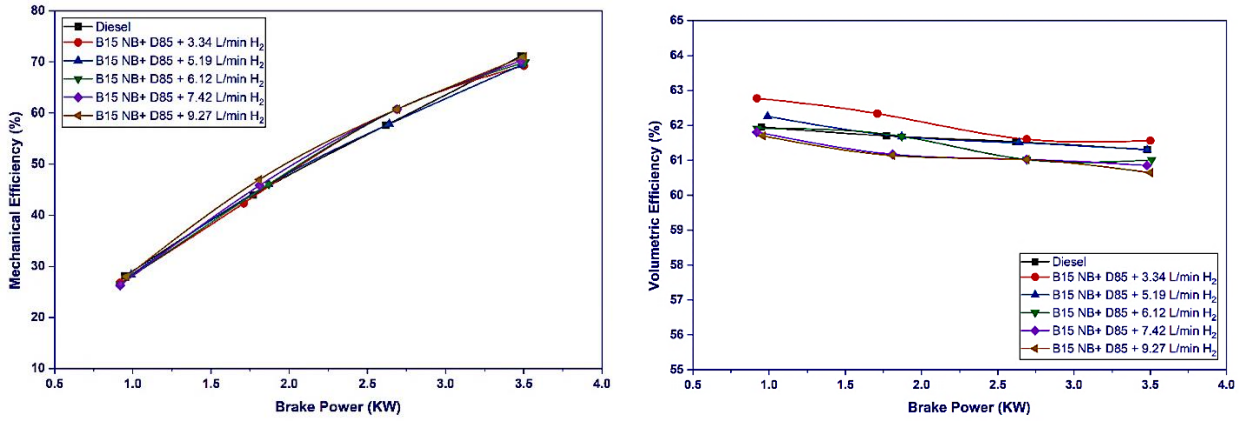

(a) Mechanical efficiency (b) Volumetric efficiency

Figure 11. Efficiency variations for different hydrogen flow rates and Neem biodiesel-diesel fuel combinations

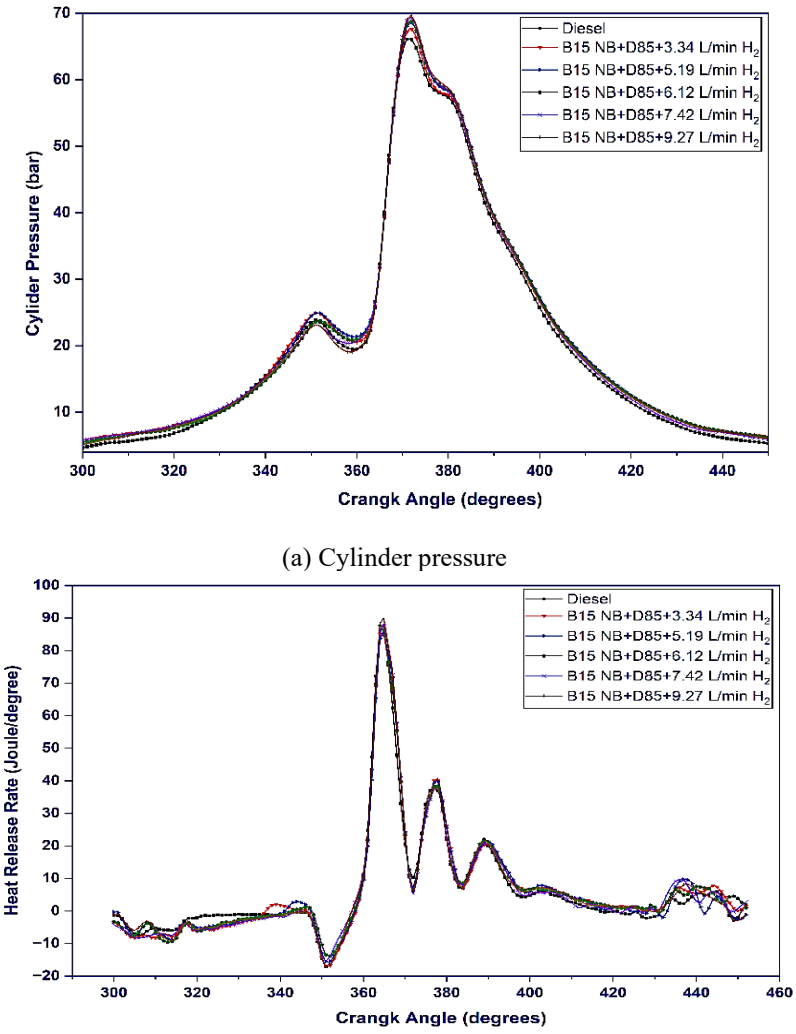

(a) Cylinder pressure

(b) Heat release rate

Figure 12. Variation of cylinder pressure and heat release rate for hydrogen supply and Neem biodiesel-diesel fuel combinations

Figure 12(a) illustrates the variation of cylinder pressure with crank angle for diesel and B15 Neem biodiesel, operated at different hydrogen flow rates at full load. The addition of hydrogen results in a higher peak cylinder pressure than with diesel, with a progressive increase as the hydrogen flow rate increases, primarily due to hydrogen's high flame speed and superior calorific value. Diesel exhibits a peak pressure of 66.05 bar at 371° ATDC, whereas hydrogen flow rates of 3.34, 5.19, 6.12, 7.42, and 9.27 L/min produce peak pressures of 67.61, 68.61, 68.76, 69.28, and 69.54 bar, respectively. The delayed combustion onset in diesel is attributed to its longer ignition delay relative to hydrogen-enriched operation. Figure 12(b) presents the variation of heat release rate with crank angle for diesel and hydrogen-enriched operation at full load. All hydrogen flow rates exhibit combustion behavior like diesel, with minor shifts in peak magnitude and crank angle location. The maximum heat release rate increases from 86.45 J/°CA for diesel to 89.12 J/°CA at a hydrogen flow rate of 9.27 L/min, owing to hydrogen's higher heating value and faster flame propagation. The negative heat release region corresponds to the compression and pre-combustion phase caused by fuel vaporization and heat loss to the cylinder walls. Overall, hydrogen enrichment with Neem biodiesel enhances combustion efficiency with only marginal changes in heat release characteristics.

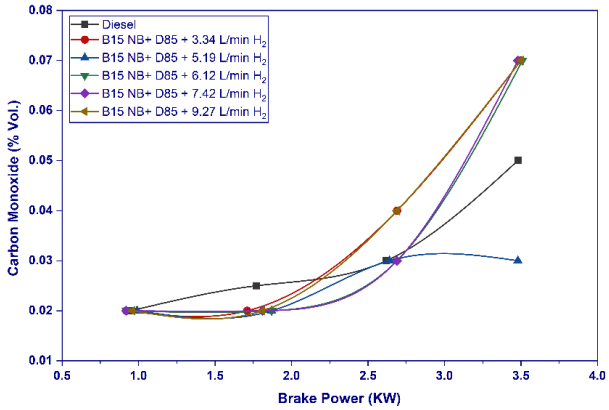

(a) Carbon monoxide

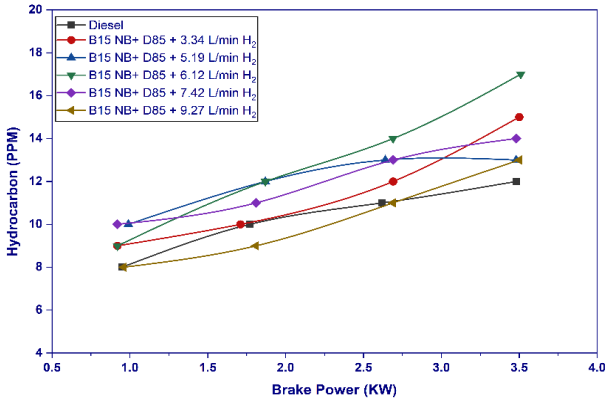

(b) Hydrocarbons

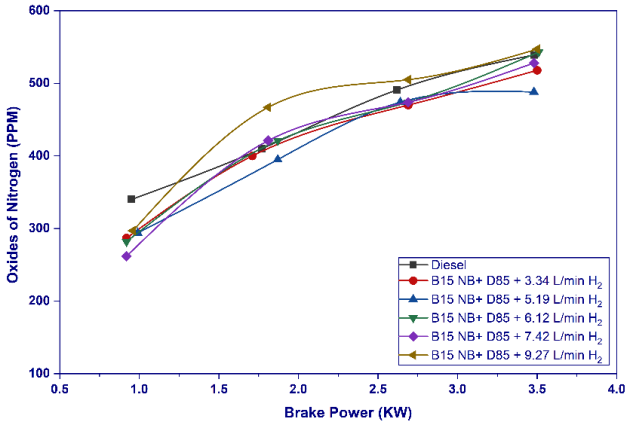

(c) Nitrogen oxides

Figure 13. Emission variations for different hydrogen flow rates and Neem biodiesel-diesel fuel combinations

3.4 Evaluation of Emission Parameters of CI Engine for Varying Hydrogen Flow Rate, Optimum Biodiesel Blend, and Diesel Fuel

Similarly, emission parameters were evaluated at the optimum Neem biodiesel blend and at different hydrogen gas flow rates (3.34, 5.19, 6.12, 7.42, and 9.27 L/min) across varying load conditions. As depicted in Figure 13(a), CO emissions increase with brake power for all hydrogen-enriched conditions and diesel fuel, primarily because incomplete combustion occurs at higher load conditions. The lowest CO emissions are produced by B15 Neem biodiesel with a hydrogen supply of 5.19 L/min at 0.04%. It shows good fuel combustion. However, when the hydrogen supply is increased from 6.12 to 9.27 L/min, the CO emissions increase further. It happens because there is an ad available for combustion. These results show that it is important to carefully add hydrogen to improve combustion and reduce emissions, such as CO. The trend in Figure 13(b) shows that HC emissions increase with brake power across all fuel combinations. This happens because at higher brake power, more fuel is injected, which causes incomplete combustion. Also, the rich mixture zones during combustion lead to higher HC emissions. The B15 Neem biodiesel with 6.12 L/min of hydrogen gives the highest HC emissions at 17 PPM. It is because of poor air-fuel mixing and delayed ignition. On the other hand, the blend with 5.19 L/min of hydrogen consistently has the lowest HC emissions at 13 PPM because hydrogen's faster flame speed helps to burn fuel more effectively. These results also show that adding hydrogen can minimize HC emissions, but optimizing the

hydrogen flow rate is also required. Figure 13(c) shows NOx emissions for the optimum Neem biodiesel blend and diesel fuel at different hydrogen flow rates. It is found that as the inside cylinder temperature increases with brake power, the NOx emissions also increase. The NOx level is at a maximum of 547 PPM with a hydrogen flow of 9.27 L/min. This is due to the addition of more hydrogen, which speeds up combustion and produces more energy. At the hydrogen flow rate of 5.19 L/min, NOx emissions are lowest at 488 PPM. This suggests that the optimal amount of hydrogen helps the engine burn more cleanly at moderate power levels.

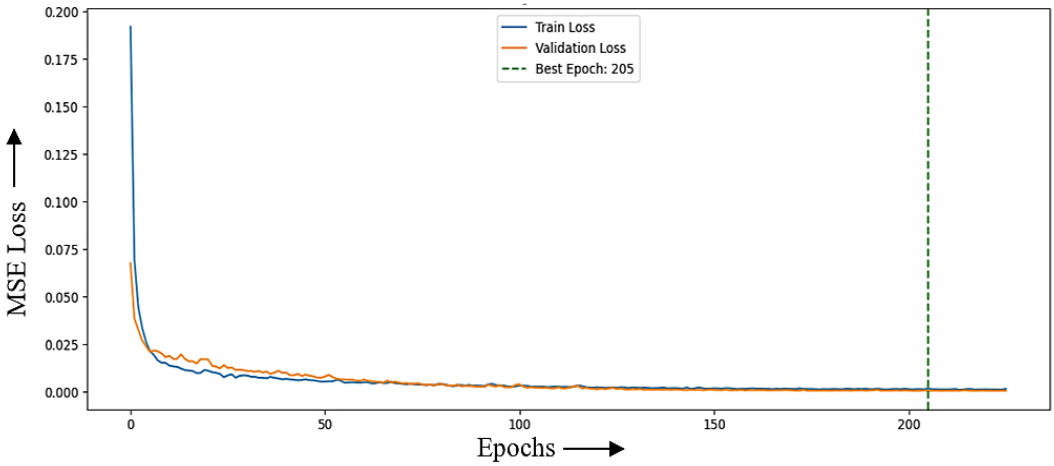

Figure 14. Training and validation loss convergence of the ANN model

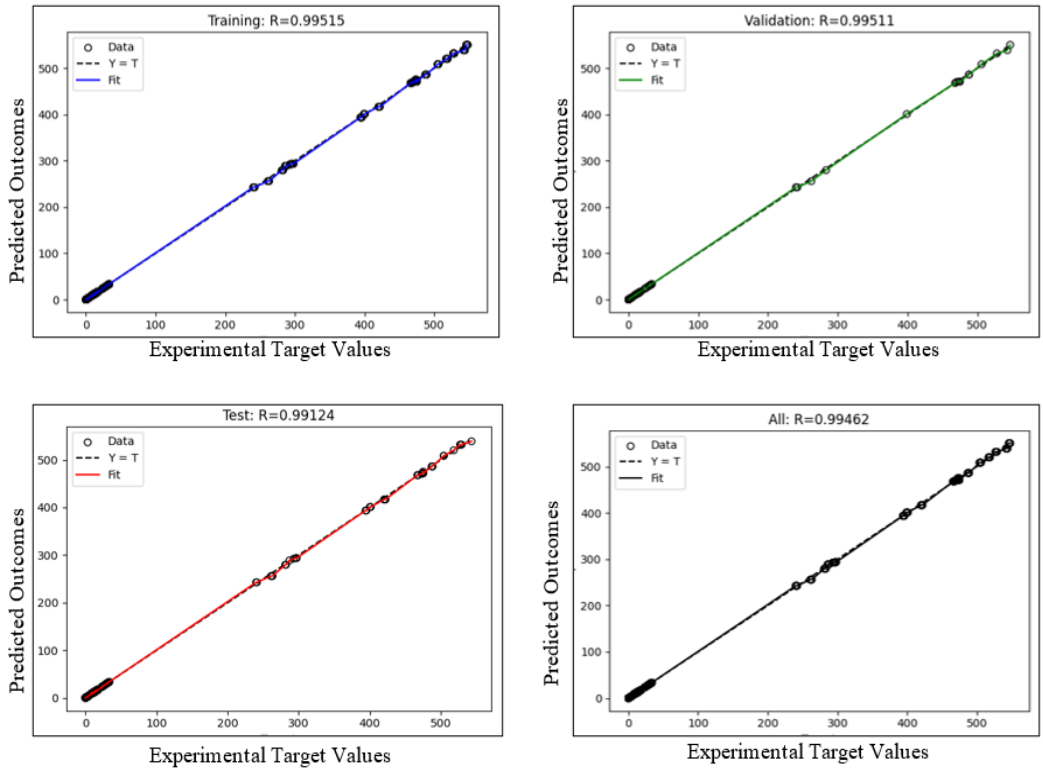

Figure 15. The overall R-values of the ANN model for training, validation, testing, and complete datasets

3.5 Performance Metrics and Model Optimization

To evaluate the effectiveness of the trained ANN model, statistical parameters like MSE, MAPE, the Correlation Coefficient (R), and the Coefficient of Determination (R^2) are used. A thorough assessment of these measures across the training, validation, and test datasets was conducted to yield insights into the model's accuracy and generalization. As shown in Figure 14, a reduction in mean squared error is observed at the 205th training epoch for both the training and validation datasets, indicating effective ANN learning. The MSE decreased significantly at first, but it slowly levelled off as the model converged. The 205th epoch, indicated by the green dotted line, had the lowest validation error, indicating it was the best at predicting new data. The model trained successfully because the MSE values were low and similar across multiple datasets, indicating it did not overfit or underfit. The fact that the training and validation results are very similar shows that the model's structure and settings are working well. The continuously low mean-squared error across all datasets indicates that the model accurately forecasts the performance parameters and emissions of the CI engine under

diverse operating situations. The ANN model performs well, as shown in Figure 15. The R-values (regression coefficients) are 0.99515 during training, 0.99511 during validation, and 0.99124 on the test set. The overall R-value is 0.99462. These numbers show that the model's predictions are quite close to the real data. It is good for finding specific patterns accurately. It works well with varied datasets, indicating that the ANN is a good choice for accurate predictions in this case [27, 29]. The study used the Leaky ReLU activation function and evaluated the model's performance using several key metrics: MSE, MAPE, and R^2 across training, validation, and test datasets. The MSE scores were 2.67 for training, 7.19 for validation, and 2.94 for testing, indicating low error levels across all phases. The MAPE values stood at 1.93%, 2.22%, and 2.43%, respectively, indicating strong predictive accuracy. The R^2 scores achieved were 0.99 during the training phase and 0.98 for validation and testing. These results demonstrate strong alignment with the data, indicating the model's ability to generalize effectively and deliver reliable performance on unseen datasets.

Figure 16 presents the test results for BTE and BSFC, along with predictions from an ANN. In Figures 16(a-b), compare the experimental BTE data with the ANN's estimates. The results are closely aligned, with an R^2 of 0.99946, MSE of 0.01885, and MAPE of just 0.42%. Similarly, Figures 16(c-d) show the actual BSFC values against the ANN predictions. These figures reveal an R^2 of 0.99354, an MSE of 0.00004, and a MAPE of approximately 1.51%, indicating strong agreement between the measurements and the model's predictions.

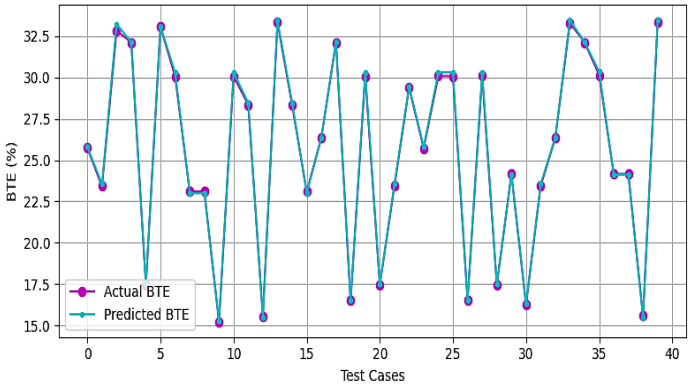

(a) Comparison of experimental and predicted BTE

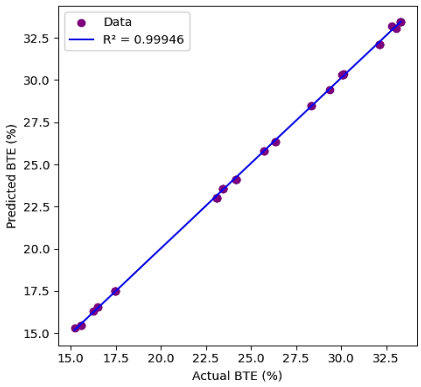

(b) Regression analysis for BTE

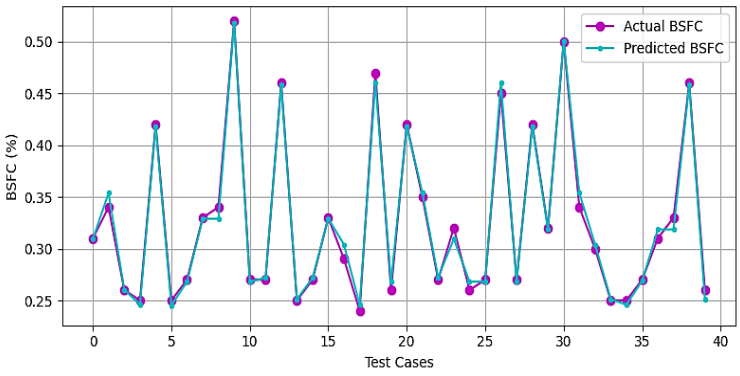

(c) Comparison of experimental and predicted BSFC

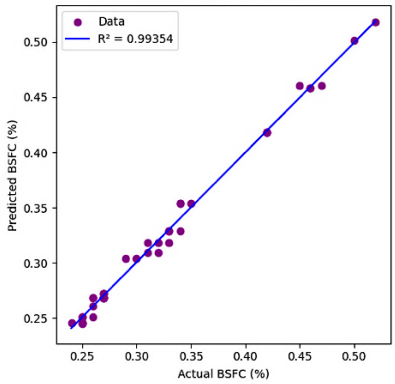

(d) Regression analysis for BSFC

Figure 26. Artificial Neural Network prediction accuracy for engine performance: (a) comparison of experimental and predicted BTE, (b) regression analysis for BTE, (c) comparison of experimental and predicted BSFC, and (d) regression analysis for BSFC

3.6 Comparative Analysis with The Literature

In the present work, using B15 Neem biodiesel fuel combined with hydrogen at the optimal flow rate of around 5.19 L/min showed the best overall performance. It enhanced engine performance and lowered CO and HC emissions. These results align well with previous research indicating that adding hydrogen to biodiesel can improve the efficiency of CI engines [20, 29]. The statistics from the ANN models, including R^2, MSE, MAPE, and the correlation coefficient (R), align closely with findings reported in existing studies [12, 27, 30]. An R^2 value of 0.9998 indicates that the model forecasts outcomes with exceptional precision. Similarly, low MSE and MAPE values indicate that the predictions are reliable and precise. The high correlation coefficients confirm the ANN's effectiveness in modeling nonlinear relationships between engine performance and emissions. Overall, these consistent results reinforce the suitability of ANN as a valuable tool for predicting CI engine performance.

4. Conclusions

The two phases of experimental testing on a CRDI diesel engine, which consist of testing of Neem biodiesel blends and hydrogen enrichments, led to important conclusions:

- The engine's best performance with Neem biodiesel blends was observed with the B15 blend at the highest engine load.
- At B15, the maximum BTE achieved was 31.38%, reducing BSFC to 0.27 kg/kWh.
- As brake power increased, mechanical efficiency improved; however, volumetric efficiency declined slightly across all fuel blends.
- Across all fuel blends, HC, CO, and NOx emissions consistently increased with increasing brake power; however, the B15 blend consistently produced lower emissions than standard diesel.
- With the addition of optimum hydrogen gas at 5.19 L/min, BTE increased by 1.93%, and BSFC decreased by 0.02 kg/kWh compared to the engine running on optimum biodiesel fuel.
- Although NOx emissions tend to increase with hydrogen induction, the lowest NOx concentration was observed at the optimal hydrogen flow rate, suggesting an optimal enrichment threshold. However, exhaust after-treatment systems can be successfully used to lower it.
- The ANN model demonstrated excellent predictive ability, as indicated by its very low MSE and MAPE. It also had consistently strong correlation coefficients (R) and R^2 values across all datasets, indicating stability and trustworthiness.
- The model is effective at predicting the CI engine's performance across different conditions.
- Thus, an optimal blend of Neem biodiesel and an optimal hydrogen flow rate in a dual-fuel mode can be practically used in a CI engine as a better alternative to fossil fuels.

Acknowledgements
The author would like to thank Apex Innovation Pvt. Ltd. in Sangli, Maharashtra, India, for providing testing facilities and measuring the fuel properties of Neem biodiesel.

Funding
This study was not supported by any grants from funding bodies in the public, private, or not-for-profit sectors.

Declaration of Competing Interest
The author declares no conflicts of interest.

CRediT Authorship Contribution Statement
Dattatray S. Doifode: Conceptualisation, Validation, Formal analysis; Data curation, Writing - original draft, Visualisation.
Ashok J. Keche: Methodology, Project administration, Writing - review & editing, Supervision.

Availability of Data and Materials
The data supporting this study's findings are available on request from the corresponding author.

Ethics Declarations
This study did not involve human participants or animals. Ethical approval was therefore not required.

Generative Artificial Intelligence Declarations
The authors claim that artificially intelligent-assisted technologies, such as generative AI, were not used to generate content, ideas, or theories. We have just utilised AI to enhance readability and refine the language. This was used with extreme human control and oversight. The authors take full responsibility for reviewing and approving the content.

References
[1] K. Maniyar, G. Kale, A. Salunke, A. Salunke, R. Marode, P. Jadhav, et al., "Comparative study of hybrid vehicles with traditional vehicles," in *Green Technology and Smart Materials for Engineering Applications*, CRC Press, 2025, pp. 385–396.
[2] S. Sayyed, R.K. Das, K. Kulkarni, "Experimental investigation for evaluating the performance and emission characteristics of DICI engine fueled with dual biodiesel-diesel blends of Jatropha, Karanja, Mahua, and Neem," *Energy*, vol. 238, p. 121787, 2022.
[3] E. Elnajjar, S.A.B. Al-Omari, M.Y.E. Selim, S.T.P. Purayil, "CI engine performance and emissions with waste cooking oil biodiesel boosted with hydrogen supplement under different load and engine parameters," *Alexandria Engineering Journal*, vol. 61, no. 6, pp. 4793–4805, 2022.
[4] A. Loyte, J. Suryawanshi, S.S.K. Bellala, R.V. Marode, Y. Devarajan, "Current status and obstacles in the sustainable synthesis of biohydrogen from microalgal species," *Results in Engineering*, vol. 24, p. 103455, 2024.
[5] M.H. Ali, M. Mashud, M.R. Rubel, R.H. Ahmad, "Biodiesel from Neem oil as an alternative fuel for diesel engine," in *Procedia Engineering*, vol. 56, pp. 625–630, 2013.
[6] M. Takase, T. Zhao, M. Zhang, Y. Chen, H. Liu, L. Yang, et al., "An expatiate review of neem, jatropha, rubber and karanja as multipurpose non-edible biodiesel resources and comparison of their fuel, engine and emission properties," *Renewable and Sustainable Energy Reviews*, vol. 43, pp. 495-520, 2015.

[7] B.A. Oni, D. Oluwatosin, "Emission characteristics and performance of neem seed (Azadirachta indica) and Camelina (Camelina sativa) based biodiesel in diesel engine," *Renewable Energy*, vol. 149, pp. 725–734, 2020.
[8] D.Y. Dhande, S. J. Navale, "Experimental investigations on the performance and emissions of compression ignition engine fuelled with lower blends of neem-based biodiesel," *Archives of Automotive Engineering*, vol. 103, no. 1, pp. 57–76, 2024.
[9] M. Mathiyazhagan, K. Meenakshi Sundaram, G. Bupesh, "Production and emission evaluation of neem biodiesel blends in a single cylinder diesel engine," in *Materials Today: Proceedings*, vol. 62, pp. 2124-2132, 2022.
[10] S. Senthil, N. Poyyamozhi, R. Sathiyamoorthi, N. Dilip Raja, M. Muthukannan, "Experimental analysis of hemispherical combustion geometry of diesel engine (neem oil) biodiesel with nano additives," *Interactions*, vol. 245, no. 1, p. 258, 2024.
[11] M.M. Khan, A.K. Kadian, R.P. Sharma, S.M.M. Hasnain, A. Mohamed, A.E. Ragab, et al., "Emission reduction and performance enhancement of CI engine propelled by Neem biodiesel-Neem oil-decanol-diesel blends at high injection pressure," *Sustainability*, vol. 15, no. 11, p. 9084, 2023.
[12] S.S. Halewadimath, N.R. Banapurmath, V.S. Yaliwal, M.G. Prasad, S.S. Jalihal, M E.M. Soudagar, et al., "Effect of manifold injection of hydrogen gas in producer gas and neem biodiesel fueled CRDI dual fuel engine," *International Journal of Hydrogen Energy*, vol. 47, no. 62, pp. 25913–25928, 2022.
[13] N. Khan, B. Balunaik, S. Yousufuddin, "Performance and emission characteristics of a diesel engine with varying injection pressure and fueled with hydrogen and cottonseed oil methyl ester blends," *Materials Today: Proceedings*, vol. 5, no. 2, pp. 3369–3377, 2018.
[14] K. Ramalingam, E.P. Venkatesan, S. Vellaiyan, A. Mukhtar, M. Sharifpur, A.S.H. Md Yasir, et al., "Substitution of diesel fuel in conventional compression ignition engine with waste biomass-based fuel and its validation using artificial neural networks," *Process Safety and Environmental Protection*, vol. 177, pp. 1234–1248, 2023.
[15] S. Javed, Y.V.V. Satyanarayana Murthy, R.U. Baig, D. Prasada Rao, "Development of ANN model for prediction of performance and emission characteristics of hydrogen dual-fueled diesel engine with Jatropha Methyl Ester biodiesel blends," *Journal of Natural Gas Science and Engineering*, vol. 26, pp. 549–557, 2015.
[16] H. Dave, V. Vakharia, H. Panchal, M. I. H. Siddiqui, D. Dobrota, "ANN and Multilayer-ELM based prediction of combustion, performance and emission characteristics of a diesel engine fuelled with Diesel-DTBP blends," *Case Studies in Thermal Engineering*, vol. 72, p. 1063232025.
[17] T. Sathish, V. Mohanavel, M. Arunkumar, K. Rajan, M.E.M. Soudagar, M.A. Mujtaba, et al., "Utilization of Azadirachta indica biodiesel, ethanol and diesel blends for diesel engine applications with engine emission profile," *Fuel*, vol. 319, p. 123798, 2022.
[18] D. Sakthivadivel, P.G. Kumar, R. Prabakaran, V.S. Vigneswaran, K. Nithyanandhan, S.C. Kim, "A neem oil-based biodiesel with DEE-enriched ethanol and Al_2O_3nano additive: An experimental investigation on the diesel engine performance," *Case Studies in Thermal Engineering*, vol. 34, p. 102021, 2022.
[19] N. Khan, M. Sohail, N. Raja Srikanth, S. Azam Pasha Quadri, "Performance testing on IC engine using diesel mixed with neem castor oil," *International Journal of Engineering Research and Applications*, vol. 11, pp. 41–46, 2021.
[20] J.N. Nair, A.K. Kaviti, A.K. Daram, "Analysis of performance and emission on compression ignition engine fuelled with blends of Neem biodiesel," *Egyptian Journal of Petroleum*, vol. 26, no. 4, pp. 927–931, 2017.
[21] A.M. Abdullah, "Combined impact of hydrogen fuel, nitrogen, and EGR with waste spent lubricant oil blended diesel on common rail direct injection diesel engine under varying loads," *Journal of Umm Al-Qura University for Engineering and Architecture*, vol. 16, no. 4, pp. 911-922, 2025.
[22] V. Thanigaivelan, M. Loganathan, M. Vikneswaran, S. Venkatramanan, M. Manickam, "Effect of hydrogen and ethanol addition in cashew nut shell liquid biodiesel operated direct injection (DI) diesel engine," *International Journal of Hydrogen Energy*, vol. 47, no. 8, pp. 5111–5129, 2022.
[23] S. Ramalingam, M. DhakshinaMoorthy, S. Subramanian, "Effect of natural antioxidant additive on hydrogen-enriched biodiesel operated compression ignition engine," *International Journal of Hydrogen Energy*, vol. 47, no. 48, pp. 20771–20783, 2022.
[24] J. Paparao, S. Murugan, "Dual-fuel diesel engine run with injected pilot biodiesel-diesel fuel blend with inducted oxy-hydrogen (HHO) gas," *International Journal of Hydrogen Energy*, vol. 47, no. 40, pp. 17788–17807, 2022.
[25] M. Loganathan, V.M. Madhavan, K. Arun Balasubramanian, V. Thanigaivelan, M. Vikneswaran, A. Anbarasu, "Investigation on the effect of diethyl ether with hydrogen-enriched cashew nut shell (CNS) biodiesel in direct injection (DI) diesel engine," *Fuel*, vol. 277, p. 118165, 2020.
[26] M. Parthasarathy, J. Isaac JoshuaRamesh Lalvani, B. Dhinesh, K. Annamalai, "Effect of hydrogen on ethanol–biodiesel blend on performance and emission characteristics of a direct injection diesel engine," *Ecotoxicol Environ Saf*, vol. 134, pp. 433–439, 2016.
[27] M.M.K. Bhuiya, M.G. Rasul, M.M.K. Khan, N. Ashwath, A.K. Azad, M.A. Hazrat, "Second generation biodiesel: Potential alternative to edible oil-derived biodiesel," *Energy Procedia*, vol. 61, pp. 1969–1972, 2014.
[28] S.K. Dash, P.V. Elumalai, P.S. Ranjit, P.K. Das, R. Kumar, S. Kunar, et al., "Experimental investigation on synthesis of biodiesel from non-edible Neem seed oil: Production optimization and evaluation of fuel properties," *Materials Today: Proceedings*, vol. 47, pp. 2463–2466, 2021.

[29] P.M. Kadam, D.R. Dolas, S. Pal, S.S. Gajghate, "Impact of soybean biodiesel blends with mixed graphene nanoparticles on compression ignition engine performance and emission: An experimental and ANN analysis," *International Journal of Automotive and Mechanical Engineering*, vol. 21, no. 3, pp. 11512–11525, 2024.

[30] J. Nursyairah, H.L.N. Lau, R.I.A. Jalal, "Evaluation of Operability and Exhaust Emissions of Common Rail Direct Injection Engine using Biodiesel Blends in Moderate Cold Environment," *International Journal of Automotive and Mechanical Engineering*, vol. 21, no. 4, pp. 11893–11908, 2024.

Nomenclature

CI engine	:	CI engine: Compression ignition engine
CRDI	:	CRDI: Common rail direct injection
B15	:	B15: 15% of Biodiesel (By volume)
NB	:	NB: Neem biodiesel
D	:	D: Diesel
ANN	:	ANN: Artificial Neural Network
BTE	:	BTE: Brake thermal efficiency
BSFC	:	BSFC: Brake specific fuel consumption
HC	:	HC: Hydrocarbon
NOx	:	NOx: Oxides of Nitrogen
CO	:	CO: Carbon Monoxide
L/min	:	L/min: Liter per minute
PPM	:	PPM: Parts per million
MAPE	:	MAPE: Mean absolute percentage error
MSE	:	MSE: Mean squared error
R	:	R: Correlation coefficient
R2	:	R2: Coefficient of determination
J/°CA	:	J/°CA: Joules per degree of Crank Angle.